J. Am. Soc. Mass Spectrom. (2015) 26:631–640
DOI: 10.1007/s13361-014-1073-y

FOCUS: EMERGING INVESTIGATORS: RESEARCH ARTICLE

Quantifying Reversible Oxidation of Protein Thiols in Photosynthetic Organisms

William O. Slade,[1] Emily G. Werth,[1] Evan W. McConnell,[1] Sophie Alvarez,[2] Leslie M. Hicks[1]

[1]Department of Chemistry, University of North Carolina at Chapel Hill, Chapel Hill, NC 27599, USA
[2]Donald Danforth Plant Science Center, St. Louis, MO 63132, USA

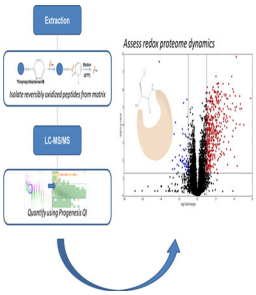

Abstract. Photosynthetic organisms use dynamic post-translational modifications to survive and adapt, which include reversible oxidative modifications of protein thiols that regulate protein structure, function, and activity. Efforts to quantify thiol modifications on a global scale have relied upon peptide derivatization, typically using isobaric tags such as TMT, ICAT, or iTRAQ that are more expensive, less accurate, and provide less proteome coverage than label-free approaches—suggesting the need for improved experimental designs for studies requiring maximal coverage and precision. Herein, we present the coverage and precision of resin-assisted thiol enrichment coupled to label-free quantitation for the characterization of reversible oxidative modifications on protein thiols. Using *C. reinhardtii* and Arabidopsis as model systems for algae and plants, we quantified 3662 and 1641 unique cysteinyl peptides, respectively, with median coefficient of variation (CV) of 13% and 16%. Further, our method is extendable for the detection of protein abundance changes and stoichiometries of cysteine oxidation. Finally, we demonstrate proof-of-principle for our method, and reveal that exogenous hydrogen peroxide treatment regulates the *C. reinhardtii* redox proteome by increasing or decreasing the level of oxidation of 501 or 67 peptides, respectively. As protein activity and function is controlled by oxidative modifications on protein thiols, resin-assisted thiol enrichment coupled to label-free quantitation can reveal how intracellular and environmental stimuli affect plant survival and fitness through oxidative stress.

Key words: Plants, Algae, Redox proteomics, Quantitative proteomics, Post-translational modifications, Oxidative stress, Reactive oxygen species

Received: 6 October 2014/Revised: 18 December 2014/Accepted: 18 December 2014/Published Online: 20 February 2015

Introduction

Reversible oxidation of protein thiols controls plant survival and fitness by regulating protein structure, function, and activity. This regulation is mediated by reactive oxygen species (ROS), which can accumulate under stress conditions and signal oxidative stress to the cell, inducing mechanisms for redox regulation. In photosynthetic organisms such as plants and algae, redox regulation is linked to antioxidants (e.g., ascorbate, glutathione), enzymes (e.g., peroxidase, catalase, superoxide dismutase), and enzyme systems (e.g., thioredoxins and glutaredoxins). Further, ROS participate in oxidative signaling by regulating protein activity of components involved in signaling cascades, therefore acting as a second messenger in stress responses. For example, nitric oxide (NO) causes S-nitrosylation of C140 on the Arabidopsis auxin receptor transport inhibitor 1 (TIR1) that promotes TIR1-AUX/IAA interaction and links nitric oxide and auxin signaling [1] in a manner that could be dependent upon crosstalk between NO and ROS [2]. In other cases, oxidative modifications play an important yet unclear role: e.g., infection of Arabidopsis by the parasitic nematode *Heterodera schachtii* stimulates the NADPH oxidases RbohD and RbohF to produce reactive oxygen species (ROS), which limits cell death and promotes infection by unknown mechanisms [3]. Thus, methods that assess the relative quantitation of oxidized thiols—defined here as redox proteomics—can reveal host-pathogen relationships as well as myriad other processes regulated by oxidative modifications that control plant survival.

Preserving the redox state of a cell requires alkylation of thiols that are reduced in vivo. When proteins are extracted

Electronic supplementary material The online version of this article (doi:10.1007/s13361-014-1073-y) contains supplementary material, which is available to authorized users.

Correspondence to: Leslie Hicks; *e-mail:* lmhicks@unc.edu

from a biological matrix, a reagent that reacts with thiols and creates an irreversible modification is included. Typical reagents include *N*-ethylmaleimide (NEM) [4] and iodoacetamide (IAM) [5]. These reagents must react with reduced thiols quickly to prevent disulfide shuffling or artefactual modification and must be thiol-specific to avoid non-specific alkylation of other nucleophilic residues. Despite the importance of free thiol blocking, few studies have defined these reaction conditions explicitly for relative quantitation in plant matrices.

Although approximately 90% of proteins in a proteome contain a cysteine, the majority of proteins (>95%) are reduced under normal growth conditions [6], with 20%–30% becoming oxidized under severe oxidative stress [5]. When these proteins are converted to peptides using trypsin in a bottom-up proteomics strategy, the proportion of peptides that contain a cysteine is low and the proportion of oxidized cysteinyl peptides can be even lower. For example, an in silico digest of the Phytozome v9.0 *C. reinhardtii* proteome using trypsin that allows one missed cleavage yields 2,425,014 peptides, of which 406,212 contain a cysteine (16.6%). If we assume that most of these peptides are reduced under normal growth conditions (95%), this leaves ~20,310 cysteinyl peptides as redox targets, or less than 1% of tryptic peptides. Thus, a requirement for a relative quantitation method for reversibly oxidized protein thiols is the enrichment of cysteinyl peptides.

Enrichment strategies for cysteinyl peptides are dominated by the biotin- or ICAT/cysTMT-switch approach in which after reduced in vivo thiols are blocked, reversibly oxidized thiols are reduced and labeled—with said label subsequently used for affinity enrichment [7–10]. Although this approach has been used to profile sites of nitrosylation in Arabidopsis [11], glutathiolylation in cyanobacteria [12], and oxidation in tomato [13], optimization of enrichment efficiency remains a key concern as background noise is high in biotin-switch assays [14] and an optimized protocol for cysTMT using a competitive elution buffer only contained 21% cysteinyl peptides [15]. Alternatively, instead of tagging oxidized thiols after reduction, affinity purification can proceed directly for the now free thiols using a disulfide exchange resin, Thiopropyl Sepharose 6B (TPS6b) [16]. Initially used to increase depth of proteome coverage for discovery experiments [17], TPS6b has recently been used for redox proteomics in cyanobacteria [18, 19] and rat myocardium [16] at enrichment efficiencies >95%.

Current strategies for quantitation using TPS6b employ peptide derivatization, typically post-enrichment, such as iTRAQ [18–20]. iTRAQ permits relative quantitation using isobaric tags with distinct reporter ions and allows multiplexing—a strategy that decreases technical variation and instrument time. Although labeled approaches are precise and fast, they yield decreased proteome coverage [21, 22], accuracy [23, 24], and linear range of quantitation [25] compared with label-free approaches, suggesting experimental designs for redox proteomics requiring maximum coverage and precision can be improved.

Herein, we present the validation of a new approach coupling TPS6b for thiol enrichment to label-free quantitation (LFQ) with improved thiol coverage and quantitative precision using *C. reinhardtii* and Arabidopsis as algae and plant model systems, respectively, for the study of reversibly oxidized thiols in photosynthetic organisms. First, alkylation conditions are examined and show protein extraction using 100 mM IAM and an incubation time of 15 min are sufficient to preserve the cellular redox state. Next, we show that our method quantifies 3662 and 1641 unique cysteinyl peptides in *C. reinhardtii* and Arabidopsis, respectively, at a level of precision compatible with label-free proteomics. Finally, we demonstrate proof-of-principle for our method, and reveal that exogenous hydrogen peroxide treatment regulates the *C. reinhardtii* redox proteome by increasing or decreasing the level of oxidation of 501 or 67 peptides, respectively. Thus, our method provides rich coverage of reversibly oxidized protein thiols and can be easily extended to include changes in protein abundance or stoichiometries of cysteine oxidation.

Methods

Cultures/Plant Material

C. reinhardtii strain CC-400 cw-15 mt+ (Chlamydomonas Resource Center) was cultivated at 22°C under 100 µmol m^{-2} s^{-1} using white light (24-h lighting) in 1 L flasks on an Innova 2300 (New Brunswick Scientific, Enfield, CT, USA) shaker at 250 rpm using Tris acetate phosphate (TAP) medium. Samples were taken at log phase with cell concentrations of 2.0×10^7 cells/mL. To examine the effects of H_2O_2 on the *C. reinhardtii* redox proteome, samples were grown to mid-log phase (1.0×10^7 cells/mL) as described above. One mM H_2O_2 was added to five biological replicates for treatment, while an equivalent volume of H_2O was added to five biological replicates for control. After 10 min, samples were immediately harvested using centrifugation and stored at –80°C until use.

Seeds of the Columbia (Col-0) ecotype of Arabidopsis were obtained from Lehle Seeds (Round Rock, TX, USA). After cold treatment for 48 h at 4°C, plants were moved to a growth chamber and grown under 100 µmol m^{-2} s^{-2} white light (8 h lighting). The growth chamber was maintained at 22°C. Rosettes were harvested pre-bolting, flash-frozen using liquid nitrogen, and stored at –80°C until use.

Protein Extraction and Blocking

Harvested *C. reinhardtii* cells were resuspended in 5-fold volume (µL mg^{-1}) of Tris-buffered phenol, pH 8.0 for 1 min (e.g., 1.5 mL of phenol per 300 mg fresh weight of cells). Homogenized cells were then mixed with 5-fold volume (µL mg^{-1}) of extraction buffer (EB): 50 mM Tris, pH 7.5, 1 mM EDTA, pH 7.5, 0.9 M Sucrose, 1% SDS, and Roche (Indianapolis, IN, USA) protease inhibitors. Frozen Arabidopsis rosettes were ground to a fine powder in liquid nitrogen and extraction proceeded as described above. For free

thiol blocking experiments, either 100 mM NEM or 100 mM IAM was also added. The mixture was incubated in the dark with agitation using a Techne (Stone, Staffordshire, UK) rotator at 10 rpm for 15, 30, 60, or 90 min. The phenol phase was separated from the aqueous phase by centrifugation at 13,000*g* and placed into a pre-chilled tube. The aqueous phase was re-extracted with an equal volume of Tris-buffered phenol, pH 8.0. Phenol phases were combined and mixed with 5-fold volume of chilled 0.1 M ammonium acetate in methanol and incubated at –80°C for at least 1 h. Precipitate was pelleted using centrifugation at 13,0000*g* and washed two times using 0.1 M ammonium acetate in methanol and once using 70% methanol. The precipitate was resuspended in 50 mM Tris, pH 7.5, 8 M urea, 0.5% SDS, and protein content was estimated using the 2D-Quant Kit (GE Healthcare, Piscataway, NJ, USA).

Protein Digestion and Reduction

Protein lysates were diluted using 50 mM Tris, pH 8.0 to achieve a urea concentration of 1.6 M. Trypsin (T6567; Sigma, St. Louis, MO, USA) was added in a 1:50 enzyme:substrate ratio and the lysates were incubated in a Thermomixer at 1000 rpm at 37°C for 12 h. Oxidized thiols were reduced using 10 mM DTT and incubated for 1 h at 37°C in a Thermomixer at 1000 rpm.

Solid-Phase Extraction

After reduction, samples were acidified using 0.5% TFA and excess DTT was removed using solid-phase extraction. tC18 50 mg sep-pak cartridges (Waters, Milford, MA, USA) were prepared by washing with 1 mL of methanol, 1 mL of 70% MeCN/30% H_2O/0.1% TFA, and 5 mL of 97% H_2O/3% MeCN/0.1% TFA. Digested protein lysates were centrifuged and then applied to the cartridge at 1 drop s^{-1} three times. Cartridges were then washed using 5 mL of 97% H_2O/3% MeCN/0.1% TFA. Peptides were eluted from the cartridge using 1.5 mL of 70% MeCN/30% H_2O/0.1% TFA. Acetonitrile was removed using a speed-vac. Samples were resuspended in 100 mM Tris-HCl, pH 7.5, 1 mM EDTA, pH 7.5, 0.5% SDS prior to enrichment.

Enrichment of Cysteinyl Peptides

For enrichments using Thiopropyl Sepharose 6b (GE Healthcare, Piscataway, NJ, USA) all solvents were degassed and the resin pelleted using centrifugation at 1500*g* for 1 min. All binding and washing steps using the resin were performed using a Techne rotator at 10 rpm and room temperature. To prepare the TPS6b for enrichment, 35 mg of the resin was rehydrated using 1 mL of H_2O at room temperature for 15 min. The resin was then washed five times each using 1 mL of H_2O and 1 mL of 100 mM Tris-HCl, pH 7.5, 1 mM EDTA, pH 7.5. Samples were applied to the resin and incubated for 2 h. The resin was washed twice using 100 mM Tris-HCl, pH 7.5, 1 mM EDTA, pH 7.5, 0.5% SDS for 15 min each, five times using 80% MeOH, 0.1% TFA for 5 min each, and eight times using 100 mM Tris-HCl, pH 7.5 for 5 min each. Bound peptides were eluted from the resin using 300 µL of 20 mM DTT in 10 mM Tris, pH 7.5 for 15 min three times. Excess DTT was removed using SPE as described earlier.

LC-MS/MS

Eluted peptides were vortexed in 97% H_2O/3% MeCN/0.1% TFA containing 10 mM DTT for 10 min. After centrifugation at 15,000*g* for 5 min, samples were transferred to total recovery 12 × 32 mm vials (Waters). Samples were analyzed using a NanoAcquity (Waters, Milford, MA, USA) coupled to a TripleTOF 5600 MS/MS (AB SCIEX, Framingham, MA, USA). Each sample was loaded onto a trap column (NanoAcquity UPLC 2G-W/M Trap 5 µm Symmetry C18, 180 µm × 20 mm) at a flow rate of 5 µL min^{-1} for 5 min. Peptides were separated using a C18 column (NanoAcquity UPLC 1.8 µm HSS T3, 75 µm × 250 mm) at a flow rate of 300 nL min^{-1}. Mobile phase A consisted of H_2O and 0.1% formic acid, and mobile base B consisted of 0.1% formic acid in MeCN. Peptides were separated using a 90-min linear gradient from 5% B to 30% B. The mass spectrometer was operated in positive ionization and high sensitivity mode. The MS survey spectrum was accumulated from a mass range of 380 to 1250*m/z* in 250 ms. For information dependent acquisition (IDA) MS/MS experiments, the first 20 features above 150 counts threshold and having a charge state of +2 to +5 were fragmented using rolling collision energy ±5%, with 100 ms spectra accumulation/experiment. Each MS/MS experiment put the precursor *m/z* on a 75 s dynamic exclusion list. Auto calibration was performed every four samples (8 h) to assure high mass accuracy in both MS and MS/MS acquisition.

Protein Inference and Data Analysis

TripleTOF 5600 raw data were converted to mascot generic format (.mgf) using MS Convertor using the Protein Pilot algorithm (AB SCIEX). Protein identifications were obtained utilizing a Mascot Server v.2.2.2 (Matrix Science, Inc., Boston, MA, USA) search engine using the *Chlamydomonas* Phytozome V9.0 database (http://www.phytozome.net/, Dec. 2012) appended with the NCBI chloroplast and mitochondrion databases (19,603 sequences total) or the Arabidopsis protein database (NCBInr 20100131; 33,343 sequences total). Searches of MS/MS data used a trypsin protease specificity and the possibility of one missed cleavage, peptide/fragment mass tolerances of 15 ppm/0.1 Da, and variable modifications of acetylation at the peptide n-term, carbamidomethylation at cysteine, oxidation at methionine, and deamidation at asparagine or glutamine. For NEM blocking studies of in vivo thiols, variable modifications included acetylation at peptide N-term, deamidation at asparagine or glutamine, oxidation at methionine, and NEM at cysteine, histidine, or lysine. To search for IAM misalkylations, variable modifications included carbamidomethylation at aspartate, glutamate, histidine, serine, threonine, lysine, or peptide N-term.

Raw (.wiff) files were imported into Progenesis QI. Automatic reference assignment and alignment of spectra was performed. Alignment was visually validated (≥80% score) and additional vectors were not needed. Peak picking parameters were set to Automatic and 5, the abundance threshold was set to 0, and exported peaklists from Progenesis QI were interrogated against the *C. reinhardtii* or Arabidopsis databases as described above. An ion score cutoff of 20 was set and an exported XML file reimported into Progenesis QI for alignment of peptide quantitation and identification. After this alignment, peptide and protein measurements were exported as .csv files and exploratory and statistical data analysis was performed using Python and R. Data normalization was not performed and analysis was performed using raw abundances. We chose to forego data normalization here as the distributions among runs were similar and we wanted to assess how our enrichment procedure affects coefficient of variation (CV) statistics, not the effect of a certain data normalization procedure.

For H_2O_2 treatment and control samples, data was processed as described above using the *C. reinhardtii* database. In this case, data normalization was performed using Progenesis QI before statistical analysis. A *t*-test (two-tailed, equal variances) was performed at the peptide-level using R. *P*-values were adjusted for FDR using the method of Benjamini and Hochberg [26]. Peptides were significantly increased or decreased in level of oxidation by H_2O_2 if their fold change (defined as the average of treatment values divided by the average of control values) was >2 or <0.05 and their FDR-adjusted *P*-value was <0.05.

Results and Discussion

LC-MS Platform Coverage and Precision

To assess the qualitative and quantitative precision of our platform, we prepared a protein lysate from *C. reinhardtii*, digested those proteins to peptides using trypsin, and performed LC-MS/MS acquisitions in triplicate (Supplemental Figure 1A). Per instrumental replicate, >14,000 unique peptides were identified (Supplemental Table 1). In comparison, Muddiman and colleagues [27] reported 13,927 unique peptides from yeast using a TripleTOF and a similar acquisition and data processing workflow. A total of 18,248 unique peptides were identified, of which 11,979 were observed in all three replicates. At the unique peptide level, overlap among replicates was 64.7%, whereas overlap at the unique protein level was 73.8% (Supplemental Figure 1B). Peptide identification from data-dependent acquisition experiments relies on peptide abundance for selection and fragmentation and the resulting MS2 spectrum, and with increased complexity of sample, peak under-sampling leads to run-to-run differences. Quantitation using a peak intensity-based label-free approach offers not only higher accuracy in quantitation compared with the use of labeling approaches, but also higher precision compared with a spectral counting approach by quantifying all peaks from the MS1 chromatogram regardless of whether the peptide is identified or not in a given replicate [24, 28–30].

Next, we assessed the precision of our LFQ workflow. In comparison to our qualitative assessment of coverage where we only consider if a peptide can be identified in a replicate, here we consider if the precursor ion is quantified across all replicates, with an identification only needed in one replicate. Across three instrumental replicates, 11,515 unique peptides were quantified at an average precursor mass accuracy of 5.3 ppm and an average retention time CV of 0.4% (Supplemental Table 2). Boxplots and smooth histograms of the raw abundances among instrumental replicates were similar (Figure 1), and the mean and median %CV was 8.9% and 5.7%, respectively (Supplemental Figure 1C). These numbers compare favorably with other LFQ workflows that use area under the curve (AUC) integration: median CV of 13% in human brain [31] and 18% in urine [32]. However, these are not direct comparisons as those studies used different platforms and data processing regimes. Although this assessment does not characterize instrumental stability over time, these metrics represent a solid baseline of performance using this platform.

Extraction/Alkylation Comparison

Preserving the cellular redox state requires alkylation of thiols that are reduced in vivo, or free-thiol blocking. This blocking should be both specific (causing minimal alkylation at non-Cys residues) and fast (avoiding disulfide shuffling or artefactual oxidation). The reaction can be achieved by Michael addition using *N*-ethylmaleimide (NEM) or SN2 substitution using IAM. Some reports show the NEM reaction is complete—with misalkylation events <10%—within 1–15 min at 25°C [33], whereas others used 30 min at 50–55°C [18, 34]. In comparison, the reaction using IAM can be incomplete after 4–6 h [35, 36], yet untargeted studies have used 30 min at 25°C [5]. Initially, we compared blocking efficiency—defined as the number of observed cysteines that are labeled with blocking reagent to the total number of observed cysteines—of 100 mM IAM or 100 mM NEM after 90 min at 25°C in *C. reinhardtii* using our LFQ workflow depicted in Figure 1, with the exception that no reductant was used. With NEM-blocking, we observed 4624 cysteinyl peptides that contained 5340 cysteines. Of these, 4964 were labeled with NEM, whereas 376 were not, yielding a blocking efficiency of 93%. In comparison, with IAM we observed 3708 cysteinyl peptides containing 4285 cysteines, of which 4252 were labeled with IAM and 33 were not, yielding a blocking efficiency of 99.2%. Altough we observed more cysteines using NEM, the decrease in blocking efficiency will lead to an increased false positive rate, complicating interpretation in future analyses. Thus, we selected IAM as a blocking agent for our procedure and used it for all further experiments. To optimize the reaction time for blocking of reduced in vivo thiols in *C. reinhardtii* using 100 mM IAM, a time-course was performed in duplicate from 15 to 90 min at 25°C evaluating labeling efficiency. At 100 mM, IAM blocks reduced thiols at ≥98.9% efficiency, defined here as the number

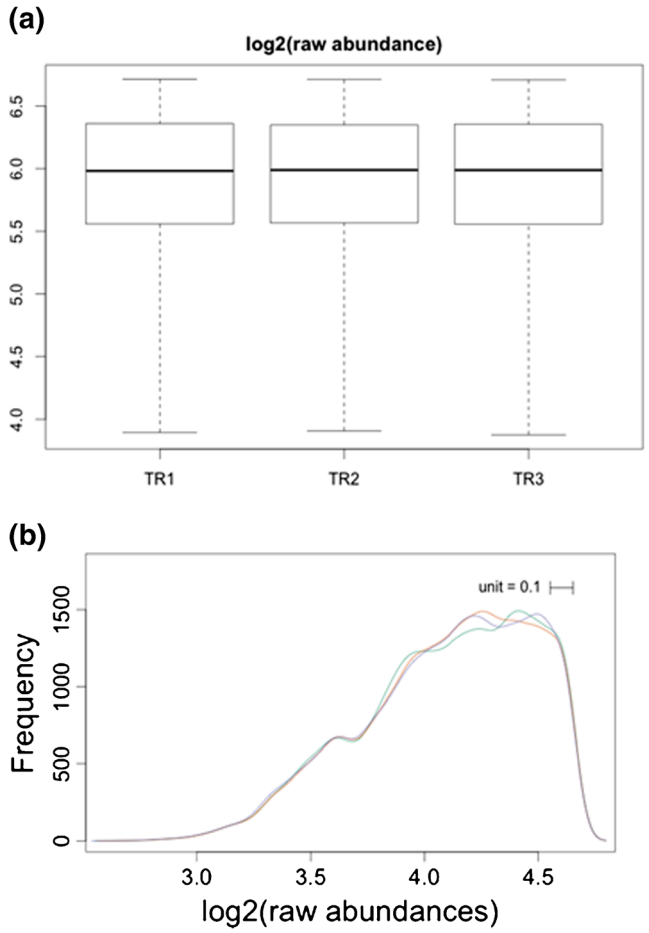

Figure 1. Boxplots and smooth histograms of raw abundances for three instrumental replicates from implemented LFQ workflow. (**a**) Boxplots without outliers and (**b**) smooth histograms in log space of raw abundances of unenriched tryptic digests of *C. reinhardtii* analyzed using LFQ workflow

of cysteinyl peptides that are blocked to the total number of cysteinyl peptides, independent of reaction time (Table 1). Additionally, we observed <1.5% misalkylation events, defined as a cysteinyl peptide containing carbamidomethylation at aspartate, glutamate, histidine, serine, threonine, lysine, or the peptide N-terminus to the number of cysteinyl peptides. These results suggest that protein extraction using 100 mM IAM and an incubation time of 15 min is an efficient method to take an in vivo snapshot of the cellular redox state in plants.

Table 1. Descriptive Statistics for 100 mM IAM Alkylation Time-Course Performed in Duplicate in *C. reinhardtii*. Enrichment Efficiency % is Defined as the Percentage of Cysteinyl Peptides Identified to the Total Number of Peptides Identified after Enrichment. Percent Misalkylation Events are Defined as the Number of IAM Derivatives at Sites Other than Cysteine to the Total Number of Peptides Identified

Time (min)	% Enrichment efficiency	% Misalkylation events
15	99.3	1.2
30	99.3	1.3
60	99.2	1.3
90	98.9	1.5

Enrichment Coverage and Precision

After protein extraction and blocking, thiols that are reversibly oxidized in vivo are reduced using dithiothreitol (DTT) and captured using a disulfide exchange resin, Thiopropyl Sepharose 6b (TPS6b). TPS6b yields excellent coverage (>1000 cysteinyl peptides) when coupled to label-free or tagged quantitation in cyanobacteria and rat myocardium [16, 18]. Here, we evaluated coverage, efficiency, and precision of TPS6b in photosynthetic cells/tissues coupled to label-free MS by splitting protein lysates of *C. reinhardtii* or Arabidopsis into the three or five 0.5 mg aliquots and performing separate enrichments (Figure 2). Using our qualitative workflow, we identified >5000 unique Cys-containing peptides in *C. reinhardtii* in three replicates at >98% enrichment efficiency, which we define as the ratio of Cys-containing peptides identified to total peptides identified (Supplemental Table 3). In Arabidopsis, we identified >1000 unique cysteinyl peptides at 84.8%–90.2% enrichment efficiency across five enrichment replicates (Supplemental Table 4). In comparison, TPS6b coupled to LFQ identified 1988 unique peptides in rat myocardial tissue at 94% enrichment [16], whereas TPS6b coupled to iTRAQ identified 670 nitrosylated peptides in cyanobacteria at >95% enrichment [18].

Experimental design and use requires an understanding of how a method affects measurement variability or precision. For example, a precision of 20% CV in a binary comparison requires five independent replicates of treatment and control to assess fold changes ≥2 at a power of ≥0.9 [37]. Here, we assessed precision using our LFQ workflow, where only peptides with a raw abundance value >0 among all enrichment are considered. Using this workflow, in *C. reinhardtii* across three enrichment replicates, we quantified 5727 cysteinyl peptides, of which 3662 were unique (Supplemental Table 5). We calculated CV distributions using raw abundances (not normalized). The distribution shows a mean of 23.8% and median of 13%, with 80% of peptides having a CV of ≤32.6%. These numbers cannot be compared with studies using isobaric tags, as those specific results were not published. But, our precision can be compared with other enrichment strategies for PTMs in comparable matrices that use LFQ post-enrichment. For example, in rat brain, Soderblom et al. characterized phosphopeptide enrichment using TiO_2 and observed that 80% of phosphopeptides had a CV of less than 33%, with median CVs of 23.4% and 19.7% for singly and multiply phosphorylated peptides, respectively [38].

Although *C. reinhardtii* is an excellent model system, our strain lacks a cell wall, and we wanted to ensure our extraction and enrichment is robust with different plant matrices. We chose Arabidopsis as a model plant as it contains a cell wall, contains 30%–60% RuBiSCo depending upon the tissue, and a plethora of secondary metabolites, all of which could complicate extraction, blocking, and enrichment. In Arabidopsis, across five enrichment replicates, we quantified 2641 cysteinyl peptides, of which 1641 are unique (Supplemental Table 6). The CV distribution using raw abundances shows a mean of

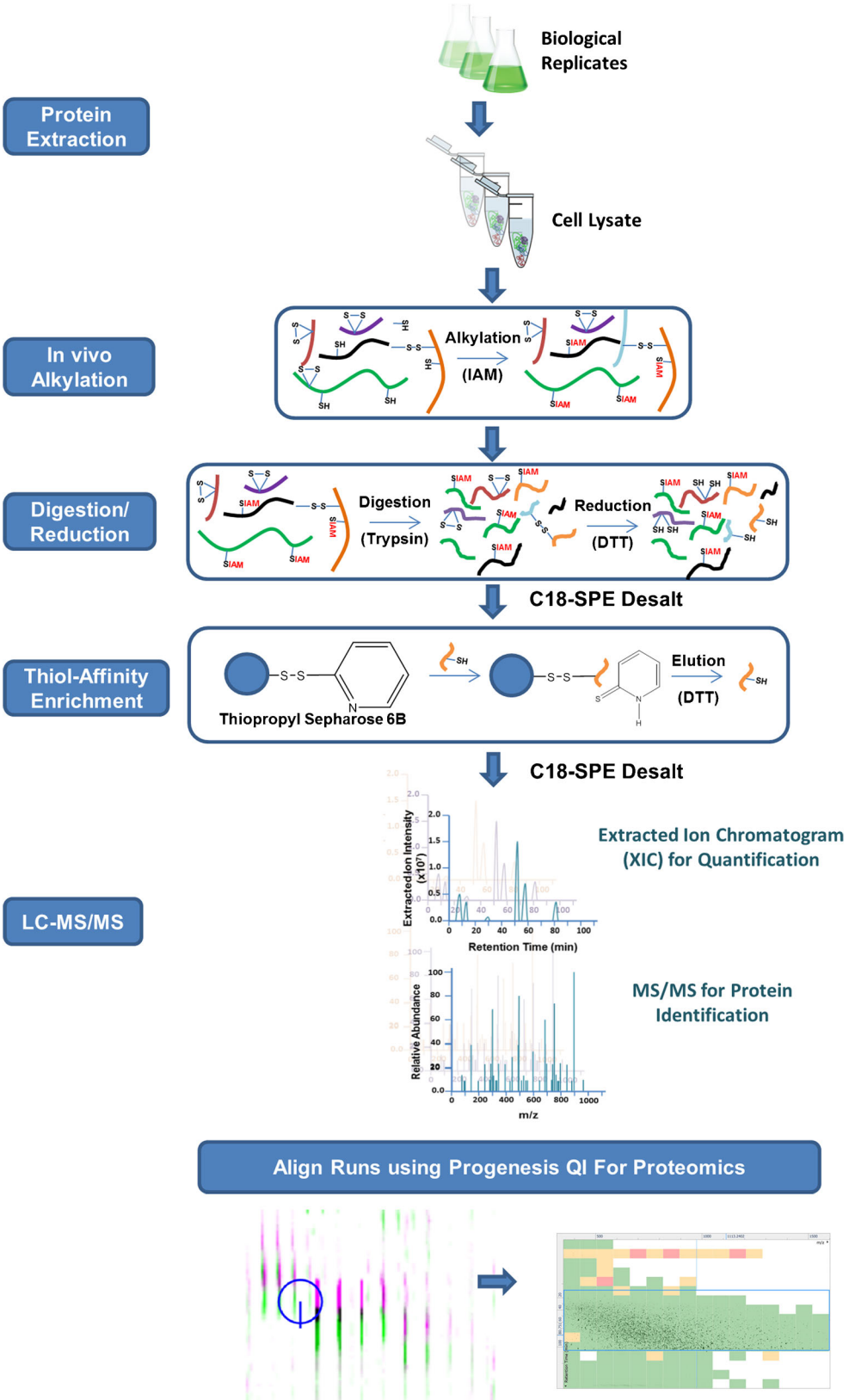

Figure 2. Overview of our template workflow for label-free quantitation coupled to resin-assisted enrichment. During the protein extraction, blocking of reduced in vivo thiols occurs using IAM. Proteins are then digested using trypsin and reduced using DTT prior to enrichment. TPS6b captures reduced thiols via disulfide exchange. Enriched peptides are eluted using DTT and processed using C18-SPE. After LC-MS/MS, raw data is imported into Progenesis QI for accurate mass and retention time (AMRT) alignment and quantitation by area under the curve (AUC) integration

22% and median of 16%, with 80% of peptides having a CV ≤27.4%. In comparison, an OxITRAQ approach surveyed 1098 cysteinyl peptides in Arabidopsis across two biological replicates at a combined analytical and biological precision of <5% [39]. This is consistent with the observed difference between label-free and labeled approaches: an increase in precision and throughput using labels comes at the cost of decreased coverage.

To test if a subset of enriched peptides were associated with higher variability, we compared enriched peptides having CV values less than 40% to those having CV values greater than 40%. We used ESP predictor [40], software that aids in the selection of peptides for selected-reaction monitoring (SRM) assays, to calculate a variety of physiochemical properties, combined these results with the output from Progenesis, and compared frequency distributions. Using this qualitative approach, we do not observe clear trends across Arabidopsis and *C. reinhardtii* (Supplemental Figures 2 and 3), suggesting TPS6b is not more variable for certain peptides.

To assess if TPS6b is biased towards peptides of certain physiochemical properties, we compared histograms of the peptide properties calculated using ESP predictor from our platform assessment (unenriched) and from our TPS6b enrichment (enriched). We chose our unenriched samples as the background to account for any intrinsic biases of our platform. We only observed a slight bias against peptides with an isoelectric point >9 (Figure 3). To assess if this bias is due to our method or a property of cysteinyl peptides, we used DBToolKit [41] to perform an in silico tryptic digest with the possibility of one missed cleavage of the *C. reinhardtii* proteome. We then used BioPython [42] to calculate the isoelectric points of all cysteinyl peptides from the in silico digest and our enriched samples and compared frequency distributions in log space (Figure 4). The distributions suggest our method is slightly biased for peptides containing an isoelectric point less than 9.

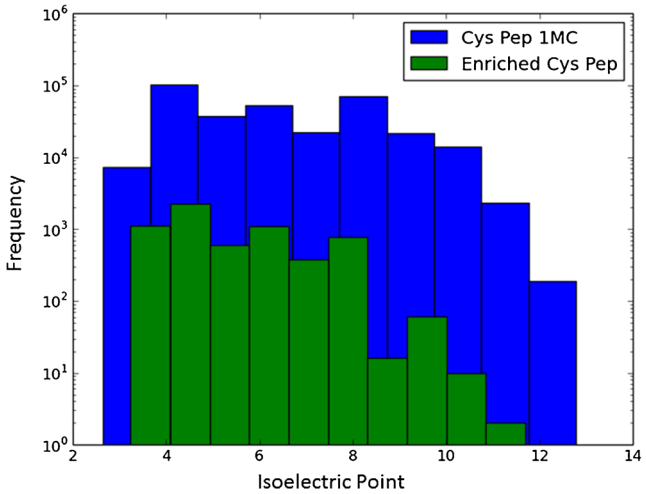

Figure 4. Comparison of isoelectric points. Isoelectric point comparison in log space of peptides containing a cysteine from: blue, an in silico digest of the *C. reinhardtii* allowing one missed cleavage, and green, peptides observed after TPS6b enrichment

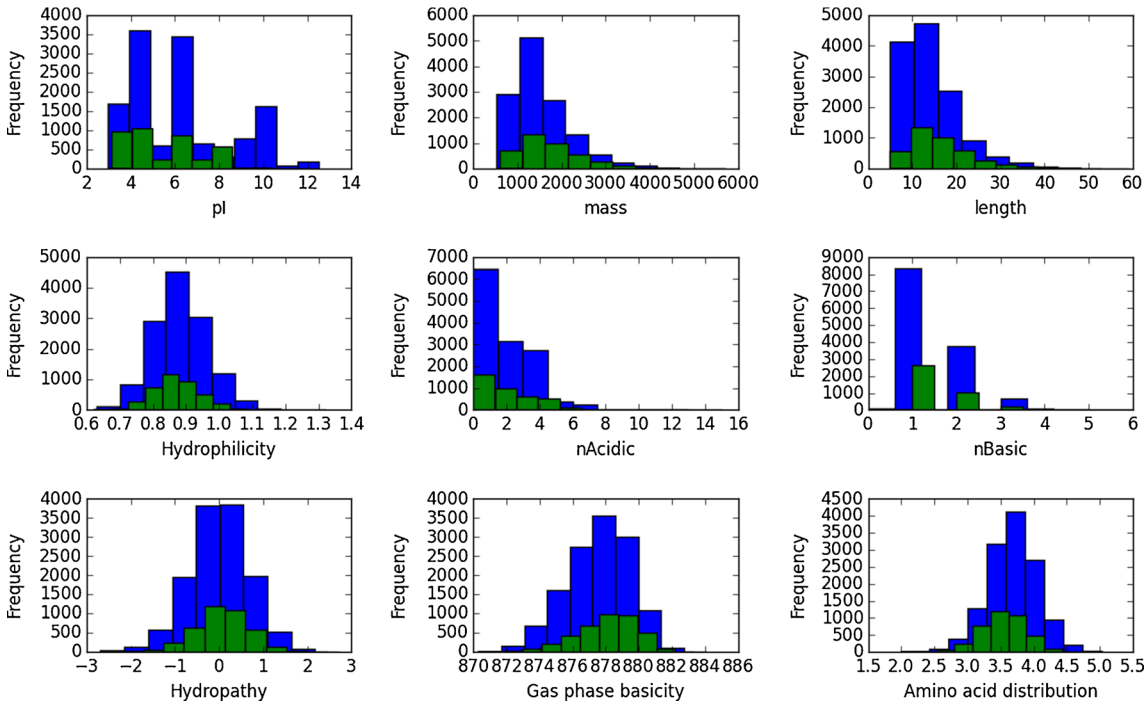

Figure 3. Comparison of peptide physiochemical properties between unenriched and enriched datasets. ESP predictor was used to calculate physiochemical properties of peptides observed between unenriched (blue, *C. reinhardtii* proteome) and enriched (green, *C. reinhardtii* redox proteome) samples

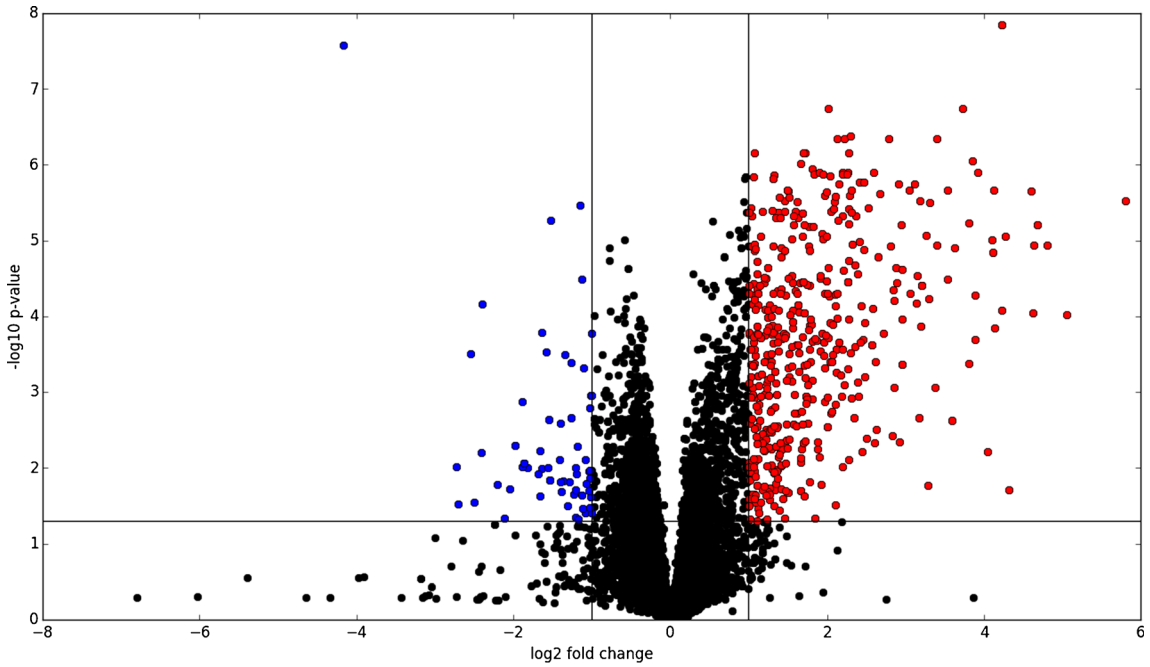

Figure 5. Volcano plot of cysteinyl peptides regulated by exogenous hydrogen peroxide in *C. reinhardtii*. Fold change is defined as the average of treatment (H_2O_2) values divided by control values across 10 biological replicates. The two vertical black lines indicate log2 fold change values of 2 and 0.5. The horizontal black line indicates an FDR-adjusted *P*-value of 0.05. Spots in red are those peptides that are increased in level of oxidation after 10 min of H_2O_2 treatment whereas those in blue are decreased

The variability induced by an enrichment procedure must be understood and controlled, when possible, to obtain meaningful and reproducible results. Our data shows TPS6b enrichment coupled to LFQ in photosynthetic organisms is capable of measuring 80% of peptides at a CV of <28%. This implies that to detect fold changes ≥1.5 at a power of 0.8, at least four independent replicates are necessary [37] . Given that our method does not require offline fractionation, a binary comparison would require approximately 24 h of instrument time, assuming 2 h per sample and calibration runs. Of course, this number does not include biological variation, which would need to be determined and would likely require additional replicates.

This method can be extended to include the detection of changes in protein abundance or stoichiometries of cysteine oxidation. The most efficient way to address both is to prepare a sample according to our method without using a blocking agent in the extraction buffer. This will result in no discrimination between peptides that are reversibly oxidized or reduced in vivo. Thus, these peptides can serve as surrogates for protein abundance and the maximum amount of the peptide that can be reduced in vivo. Values from experiments using a blocking agent will represent the amount of oxidized peptide available and can be normalized to the amount of maximum peptide available to obtain the stoichiometry of cysteine oxidation. We evaluated the coverage and precision of this strategy in *C. reinhardtii* using TPS6b enrichment coupled to our LFQ workflow. For this experiment, we extracted proteins from *C .reinhardtii* without using a blocking agent, resulting in no discrimination between those thiols that are reduced or reversibly oxidized in vivo, and reduced protein thiols using DTT prior to enrichment. Further, we alkylated thiols using IAM after enrichment and elution using DTT. Across two enrichment replicates, we quantified 8662 cysteinyl peptides, of which 4998 are unique (Supplemental Table 7). The CV distribution using raw abundances shows a mean of 16.5% and a median of 10.9%, with 80% of peptides containing a CV <23.5%. These results demonstrate our procedure is compatible with detecting changes in protein abundance and cysteine oxidation. Thus, our method can reveal how oxidative stress controls the survival of photosynthetic organisms by characterizing both changes in protein abundance and changes in cysteine oxidation.

To demonstrate proof-of-principle for our method, we assessed the effects of exogenous hydrogen peroxide treatment on the *C. reinhardtii* redox proteome. *C. reinhardtii* was grown to mid-log phase (1.0×10^7 cells/mL) and treated using 1 mM hydrogen peroxide (five biological replicates for treatment) or water (five biological replicates for control) for 10 min. Across 10 biological replicates, we quantified 8592 cysteinyl peptides, of which 4612 have unique sequences (Supplemental Table 8). We tested if these 8592 cysteinyl peptides were affected by hydrogen peroxide by applying a *t*-test (two-tailed, equal variances). *P*-values were corrected for false-discovery rate (FDR) using the method of Benjamini and Hochberg [26]. Peptides were significantly altered if the ratio of the average of treatment values to control values was >2 or <0.5 and their FDR-adjusted *P*-value was <0.05 (Fig. 5). Using these criteria, 568 of the 8592 cysteinyl peptides were significantly regulated in abundance by hydrogen peroxide treatment. As expected, most

increased, whereas 67 decreased (Supplemental Table 8). Although counterintuitive, protein thiols decreasing in level of oxidation upon oxidative stress is documented [39, 43, 44]. Our total coverage of 8592 cysteine-containing peptides compares favorably with other methods for quantification of reversible oxidation of protein thiols: 1098 cysteinyl peptides from Arabidopsis for OxiTRAQ [39], 912 cysteinyl peptides from *E. coli* for cysTMTRAQ [45], and 2067 cysteinyl peptides from Cyanobacteria for TPS6b coupled to iTRAQ quantitation [19]. Thus, these results indicate TPS6b coupled to label-free quantification is a robust and viable alternative for the analysis of reversible oxidation of protein thiols.

Conclusions

In conclusion, we have presented the coverage and precision of TPS6b enrichment coupled to label-free quantitation in photosynthetic organisms. We demonstrate that protein extraction using 100 mM IAM and an incubation time of 15 min is sufficient to block thiols that are reduced in vivo. Further, we quantified 3662 and 1641 unique cysteinyl peptides that were oxidized in vivo in *C. reinhardtii* and Arabidopsi*s*, respectively. This quantitation occurred with only a slight bias towards peptides with an isoelectric point <9. This method can be extended to simultaneously quantify changes in protein abundance or stoichiometries of cysteine oxidation. Finally, we demonstrate proof-of-principle for our method, and show that exogenous hydrogen peroxide increases or decreases the oxidation level of 501 or 67 cysteinyl peptides, respectively, in *C. reinhardtii*. Because protein activity and function is controlled by oxidative modifications on protein thiols, TP6Sb coupled to label-free quantitation can reveal how intracellular and environmental stimuli affect plant survival and fitness through oxidative stress.

Acknowledgments

This work was supported as part of the Center for Advanced Biofuels Systems (CABS), an Energy Frontier Research Center funded by the U.S. Department of Energy, Office of Science, Office of Basic Energy Sciences under Award Number DE-SC0001295.

References

1. Terrile, M.C., Paris, R., Calderon-Villalobos, L.I.A., Iglesias, M.J., Lamattina, L., Estelle, M., Casalongue, C.A.: Nitric oxide influences auxin signaling through S-nitrosylation of the Arabidopsis transport inhibitor response 1 auxin receptor. Plant J. **70**(3), 492–500 (2012)
2. Kwak, J.M., Nguyen, V., Schroeder, J.I.: The role of reactive oxygen species in hormonal responses. Plant Physiol. **141**(2), 323–329 (2006)
3. Siddique, S., Matera, C., Radakovic, Z.S., Hasan, M.S., Gutbrod, P., Rozanska, E., Sobczak, M., Torres, M.A., Grundler, F.M.: Parasitic worms stimulate host NADPH oxidases to produce reactive oxygen species that limit plant cell death and promote infection. Sci. Signal. **7**(320), ra33 (2014)
4. Alvarez, S., Berla, B.M., Sheffield, J., Cahoon, R.E., Jez, M.J., Hicks, L.M.: Comprehensive analysis of the *Brassica juncea* root proteome in response to cadmium exposure by complementary proteomic approaches. Proteomics **9**(9), 2419–2431 (2009)
5. Garcia-Santamarina, S., Boronat, S., Domenech, A., Ayte, J., Molina, H., Hidalgo, E.: Monitoring in vivo reversible cysteine oxidation in proteins using ICAT and mass spectrometry. Nat. Protoc. **9**(5), 1131–1145 (2014)
6. Hansen, R.E., Roth, D., Winther, J.R.: Quantifying the global cellular thiol-disulfide status. Proc. Natl. Acad. Sci. U. S. A. **106**(2), 422–427 (2009)
7. Leichert, L.I., Gehrke, F., Gudiseva, H.V., Blackwell, T., Ilbert, M., Walker, A.K., Strahler, J.R., Andrews, P.C., Jakob, U.: Quantifying changes in the thiol redox proteome upon oxidative stress in vivo. Proc. Natl. Acad. Sci. U. S. A. **105**(24), 8197–8202 (2008)
8. Lindermayr, C., Saalbach, G., Durner, J.: Proteomic identification of S-nitrosylated proteins in Arabidopsis. Plant Physiol. **137**(3), 921–930 (2005)
9. Wang, Y., Feechan, A., Yun, B., Shafiei, R., Hofmann, A., Taylor, P., Xue, P., Yang, F., Xie, Z., Pallas, J.A., Chu, C., Loake, G.J.: S-nitrosylation of AtSABP3 antagonizes the expression of plant immunity. J. Biol. Chem. **284**(4), 2131–2137 (2009)
10. Murray, C.I., Uhrigshardt, H., O'Meally, R.N., Cole, R.N., Van Eyk, J.E.: Identification and quantification of S-nitrosylation by cysteine reactive tandem mass tag switch assay. Mol. Cell Proteomics **11**(2), M111 013441 (2012)
11. Fares, A., Nespoulous, C., Rossignol, M., Peltier, J.B.: Simultaneous identification and quantification of nitrosylation sites by combination of biotin switch and ICAT labeling. Methods Mol. Biol. **1072**, 609–620 (2014)
12. Chardonnet, S., Sakr, S., Cassier-Chauvat, C., Marechal, P.L., Chauvat, F., Lemaire, S.D., Decottignies, P.: First Proteomic study of S-glutathionylation in cyanobacteria. J. Proteome Res. **14**(1), 59–71 (2015)
13. Parker, J., Zhu, N., Zhu, M., Chen, S.: Profiling thiol redox proteome using isotope tagging mass spectrometry. J. Vis. Exp. **61**, e3766 (2012)
14. Santhanam, L., Gucek, M., Brown, T.R., Mansharamani, M., Ryoo, S., Lemmon, C.A., Romer, L., Shoukas, A.A., Berkowitz, D.E., Cole, R.N.: Selective fluorescent labeling of S-nitrosothiols (S-FLOS): a novel method for studying S-nitrosation. Nitric oxide Biol. Chem. Off. J. Nitric Oxide Soc. **19**(3), 295–302 (2008)
15. Qu, Z.,: Proteomic quantification and site-mapping of S-nitrosylated proteins using isobaric iodoTMT reagents. J. Proteome Res. **13**(7), 3200–3211 (2014)
16. Paulech, J.,: Large-scale capture of peptides containing reversibly oxidized cysteines by thiol-disulfide exchange applied to the myocardial redox proteome. Anal. Chem. **85**(7), 3774–3780 (2013)
17. Tambor, V.,: CysTRAQ—a combination of iTRAQ and enrichment of cysteinyl peptides for uncovering and quantifying hidden proteomes. J. Proteomics **75**(3), 857–867 (2012)
18. Guo, J.,: Resin-assisted enrichment of thiols as a general strategy for proteomic profiling of cysteine-based reversible modifications. Nat. Protoc. **9**(1), 64–75 (2014)
19. Guo, J.: Proteome-wide light/dark modulation of thiol oxidation in cyanobacteria revealed by quantitative site-specific redox proteomics. Mol. Cell. Proteomics **13**, 3270–3285 (2014)
20. Hu, Q., Guo, G., Yang, Z., Li, Y., Xia, Y., Li, N.: Stable Isotope Metabolic Labeling-Based Quantitative Thiol Redox Proteomic Analysis of Hydrogen Peroxide-treated Arabidopsis plant. J. Proteom. Bioinform. **7**(5), 121–133 (2014)
21. Wang, H., Alvarez, S., Hicks, L.M.: Comprehensive comparison of iTRAQ and label-free LC-based quantitative proteomics approaches using two *Chlamydomonas reinhardtii* strains of interest for biofuels engineering. J. Proteome Res. **11**(1), 487–501 (2012)
22. Li, Z., Adams, R.M., Chourey, K., Hurst, G.B., Hettich, R.L., Pan, C.: Systematic comparison of label-free, metabolic labeling, and isobaric chemical labeling for quantitative proteomics on LTQ Orbitrap Velos. J. Proteome Res. **11**(3), 1582–1590 (2012)
23. Ow, S.Y., Salim, M., Noirel, J., Evans, C., Wright, P.C.: Minimizing iTRAQ ratio compression through understanding LC-MS elution dependence and high-resolution HILIC fractionation. Proteomics **11**(11), 2341–2346 (2011)
24. Karp, N.A., Huber, W., Sadowski, P.G., Charles, P.D., Hester, S.V., Lilley, K.S.,: Addressing accuracy and precision issues in iTRAQ quantitation. Mol. Cell Proteomics **9**(9), 1885–1897 (2010)
25. Neilson, K.A., Ali, N.A., Muralidharan, S., Mirzaei, M., Mariani, M., Assadourian, G., Lee, A., Sluyter, S.C., Haynes, P.A.: Less label, more free: approaches in label-free quantitative mass spectrometry. Proteomics **11**(4), 535–553 (2011)
26. Benjamini, Y.A., Hochberg, Y.: Controlling the false discovery rate: a practical and powerful approach to multiple testing. J R. Stat. Soc Ser. B. Methodol. **57**(1), 289–300 (1995)

27. Andrews, G.L., Simons, B.L., Young, J.B., Hawkridge, A.M., Muddiman, D.C.: Performance characteristics of a new hybrid quadrupole time-of-flight tandem mass spectrometer (TripleTOF 5600). Anal. Chem. **83**(13), 5442–5446 (2011)
28. Tu, C., Li, J., Sheng, Q., Zhang, M., Qu, J.: Systematic assessment of survey scan and MS2-based abundance strategies for label-free quantitative proteomics using high-resolution MS data. J. Proteome Res. **13**(4), 2069–2079 (2014)
29. Hendrickson, E.L., Xia, Q., Wang, T., Leigh, J.A., Hackett, M.: Comparison of spectral counting and metabolic stable isotope labeling for use with quantitative microbial proteomics. Analyst **131**(12), 1335–1341 (2006)
30. Patel, V.J., Thalassinos, K., Slade, S.E., Connolly, J.B., Crombie, A., Murrell, J.C., Scrivens, J.H.: A comparison of labeling and label-free mass spectrometry-based proteomics approaches. J. Proteome Res. **8**(7), 3752–3759 (2009)
31. Piehowski, P.D., Petyuk, V.A., Orton, D.J., Xie, F., Moore, R.J., Ramirez-Restrepo, M., Engel, A., Lieberman, A.P., Albin, R.L., Camp, D.G., Smith, R.D., Myers, A.J.: Sources of technical variability in quantitative LC-MS proteomics: human brain tissue sample analysis. J. Proteome Res. **12**(5), 2128–2137 (2013)
32. Nagaraj, N., Mann, M.: Quantitative analysis of the intra- and inter-individual variability of the normal urinary proteome. J. Proteome Res. **10**(2), 637–645 (2011)
33. Paulech, J., Solis, N., Cordwell, S.J.: Characterization of reaction conditions providing rapid and specific cysteine alkylation for peptide-based mass spectrometry. Biochim. Biophys. Acta **1834**(1), 372–379 (2013)
34. Held, J.M., Danielson, S.R., Behring, J.B., Atsriku, C., Britton, D.J., Puckett, R.L., Schilling, B., Campisi, J., Benz, C.C., Gibson, B.W.: Targeted quantitation of site-specific cysteine oxidation in endogenous proteins using a differential alkylation and multiple reaction monitoring mass spectrometry approach. Mol. Cell Proteomics **9**(7), 1400–1410 (2010)
35. Rogers, L.K., Leinweber, B.L., Smith, C.V.: Detection of reversible protein thiol modifications in tissues. Anal. Biochem. **358**(2), 171–184 (2006)
36. Galvani, M., Hamdan, M., Herbert, B., Righetti, P.G.: Alkylation kinetics of proteins in preparation for two-dimensional maps: a matrix assisted laser desorption/ionization-mass spectrometry investigation. Electrophoresis **22**(10), 2058–2065 (2001)
37. Levin, Y.: The role of statistical power analysis in quantitative proteomics. Proteomics **11**(12), 2565–2567 (2011)
38. Soderblom, E.J., Philipp, M., Thompson, J.W., Caron, M.G., Moseley, M.A.: Quantitative label-free phosphoproteomics strategy for multifaceted experimental designs. Anal. Chem. **83**(10), 3758–3764 (2011)
39. Liu, P., Zhang, H., Wang, H., Xia, Y.: Identification of redox-sensitive cysteines in the Arabidopsis proteome using OxiTRAQ, a quantitative redox proteomics method. Proteomics **14**(6), 750–762 (2014)
40. Fusaro, V.A., Mani, D.R., Mesirov, J.P., Carr, S.A.: Prediction of high-responding peptides for targeted protein assays by mass spectrometry. Nat. Biotechnol. **27**(2), 190–198 (2009)
41. Martens, L., Vandekerckhove, J., Gevaert, K.: DBToolkit: processing protein databases for peptide-centric proteomics. Bioinformatics **21**(17), 3584–3585 (2005)
42. Cock, P.J., Anta, T., Chang, J.T., Chapman, B.A., Cox, C.J., Dalke, A., Friedberg, I., Hamelryck, T., Kauff, F., Wilczynski, B., Hoon, M.J.: Biopython: freely available Python tools for computational molecular biology and bioinformatics. Bioinformatics **25**(11), 1422–1423 (2009)
43. Wang, H., Wang, S., Lu, Y., Alvarez, S., Hicks, L.M., Ge, X., Xia, Y.: Proteomic analysis of early-responsive redox-sensitive proteins in Arabidopsis. J. Proteome Res. **11**(1), 412–424 (2012)
44. Alvarez, S., Galant, A., Jez, J.M., Hicks, L.M.: Redox-regulatory mechanisms induced by oxidative stress in *Brassica juncea* roots monitored by 2-DE proteomics. Proteomics **11**(7), 1346–1350 (2011)
45. Parker, J., Balmant, K., Zhu, F., Zhu, N., Chen, S.: cysTMTRAQ-an integrative method for unbiased thiol-based redox proteomics. Mol. Cell. Proteomics **14**, 237–242 (2015)